Dental Materials Journal 2016; 35(1): 118–125

Bioactive treatment promotes osteoblast differentiation on titanium materials fabricated by selective laser melting technology

Masako TSUKANAKA[1], Shunsuke FUJIBAYASHI[1], Mitsuru TAKEMOTO[1], Tomiharu MATSUSHITA[2], Tadashi KOKUBO[2], Takashi NAKAMURA[3], Kiyoyuki SASAKI[4] and Shuichi MATSUDA[4]

[1] *Department of Orthopaedic Surgery, Graduate School of Medicine, Kyoto University, 54 Kawahara-cho, Sakyo-ku, Kyoto 606-8507, Japan*
[2] *Department of Biomedical Sciences, College of Life and Health Sciences, Chubu University, 1200 Matsumoto-cho, Kasugai, Aichi 487-8501, Japan*
[3] *National Hospital Organization Kyoto Medical Center, 1-1 Fukakusamukaihata-cho, Fushimi-ku, Kyoto 612-8555, Japan*
[4] *Sagawa Printing, 5-3 Morimoto-cho Inui, Mukou, Kyoto 617-8588, Japan*
Corresponding author, Masako TSUKANAKA; E-mail: mtsukana@kuhp.kyoto-u.ac.jp

Selective laser melting (SLM) technology is useful for the fabrication of porous titanium implants with complex shapes and structures. The materials fabricated by SLM characteristically have a very rough surface (average surface roughness, *Ra*=24.58 μm). In this study, we evaluated morphologically and biochemically the specific effects of this very rough surface and the additional effects of a bioactive treatment on osteoblast proliferation and differentiation. Flat-rolled titanium materials (*Ra*=1.02 μm) were used as the controls. On the treated materials fabricated by SLM, we observed enhanced osteoblast differentiation compared with the flat-rolled materials and the untreated materials fabricated by SLM. No significant differences were observed between the flat-rolled materials and the untreated materials fabricated by SLM in their effects on osteoblast differentiation. We concluded that the very rough surface fabricated by SLM had to undergo a bioactive treatment to obtain a positive effect on osteoblast differentiation.

Keywords: Selective laser melting technology, Osteoblast differentiation, Bioactive treatment

INTRODUCTION

Porous titanium and its alloys are widely used in the field of orthopedic and dental surgery. Implants with porous structures on their surfaces provide high friction resistance between the host bones and have high primary stability. After implantation, the bone tissues expand into the pores, and biological fixation is achieved. A commonly used method to fabricate an implant with a porous structure on its surface is to apply a porous coating to the surface of the main body of the implant after initial manufacture. However, there are some concerns about these porous-coated implants; for example, cracking, detachment, and electrical incompatibility between the implant and the coated layer[1]. Ideally, the porous surface and the main body of the implant should be fabricated integrally as one piece. For this purpose, additive manufacturing methods with metal powders have been recently introduced to the field of orthopedics, and hip implants fabricated by electron beam melting are already in clinical use[2].

Selective laser melting (SLM) technology[3-5] is one of the additive manufacturing methods available for the formation of metal implants. In the SLM process, the small metal powder particles are melted and fused in layers by a laser. Three-dimensional (3-D) structures can be controlled using computer-aided design (CAD). This technology enables us not only to fabricate simultaneously the porous structure and the main body of the implant but also to fabricate implants with complex structures and personalized implants fitted to the defect of each patient. The clinical applications of SLM technology for reconstructive surgery have been reported for patients with facial bone defects[6,7].

Although porous titanium and its alloys have a high biocompatibility and can achieve good mechanical stability when bone has grown into the pores, they do not bond directly to living bone[8]. Various surface treatments have been developed to promote direct bonding of these materials to living bone. Examples include hydroxyapatite coating[9] and peptide immobilization[10]. Of these, bioactive treatments refer to surface treatments that promote direct bone-implant bonding by simple chemical and thermal procedures[11-13]. Orthopedic implants treated with a bioactive treatment are already available[14]. In a bioactive treatment, the material is first subjected to an alkaline or acidic treatment and then heated in a furnace. Such treatments are convenient because special equipment is not required. The additional advantages of bioactive treatments for materials fabricated by SLM are that these treatments can uniformly treat the walls of pores formed deep in the material and can induce bone into the inner pores of the material[15]. Hence, we assume that the bioactive treatments are the most suitable surface treatments for porous materials in complex shapes fabricated by SLM technology.

Because the materials are fabricated from metal powders, SLM materials characteristically have very rough surfaces with *Ra* values around 25 μm. In general, "rough" surfaces are known to have beneficial effects on bone integration[16-21]. However, in most *in vivo* and *in vitro* studies, the *Ra* values were up to 5 μm. Relatively few studies have evaluated the performance of rough surfaces with larger *Ra* values. We previously reported

Received Apr 21, 2015: Accepted Sep 2, 2015
doi:10.4012/dmj.2015-127 JOI JST.JSTAGE/dmj/2015-127

increased bone formation in rabbits for porous SLM materials that had undergone a bioactive treatment (dilute HCl-treated alkali and heat treatment)[15]. However, no *in vitro* study has evaluated the highly roughened surfaces of SLM materials combined with a bioactive treatment. Therefore, the aim of this study was to evaluate the effects of very rough surfaces of SLM materials with or without a bioactive treatment on osteoblast differentiation *in vitro*. Theoretically, it was expected that the additional application of a bioactive treatment to the very rough surfaces of SLM materials would further promote osteoblast differentiation.

In this study, primary osteoblasts harvested from neonatal mouse calvaria were cultured on three different materials: commercially available flat-rolled pure titanium (CpTi), pure titanium plates produced by SLM (SLM), and SLM materials with dilute HCl-treated alkali and heat treatment (SLM-T). Cell morphology, cell proliferation, and osteogenic differentiation of the cultured osteoblasts were evaluated by electron microscopy, immunofluorescent staining, cell-proliferation assay (XTT assay), and gene expression analysis by reverse transcriptase-polymerase chain reaction (RT-PCR).

MATERIALS AND METHODS

Preparation of materials

The flat-rolled materials were cut from commercially pure (99.5%) titanium (CpTi) plates (Nilaco, Tokyo, Japan) to a size of 14×14×1 mm and were polished with grade 400 diamond plates.

The SLM materials were fabricated as described previously[22]. Briefly, a dense cuboid sample of size 14×14×1 mm was designed using a CAD program (Magics®, Materialise, Leuven, Belgium), and the model was sliced horizontally into many thin layers of two-dimensional images. According to the data, implants were fabricated by an EOSINT M270 SLM machine (Electro Optical Systems, Krailing, Germany) using commercially pure titanium metal powder (>99.5% pure) with particle diameters of less than 45 μm (Osaka Titanium Technologies, Amagasaki, Hyogo, Japan). The process parameters for the SLM method were as follows: laser power, 117 W; scanning speed, 225 mm/s; hatch spacing, 180 μm; hatch offset, 20 μm. In this system, the laser beam had a diameter of less than 100 μm. After the SLM process, the samples were heat treated at 1,300°C for 1 h and allowed to cool naturally to room temperature. The upper side of the material was used for the evaluations.

Dilute HCl-treated alkali and heat treatment was performed according to the previously reported procedure[12,23]. First, samples were soaked in 5.0 M aqueous NaOH at 60°C for 24 h and then in 0.5 mM HCl (pH 3.4) at 40°C for 24 h, gently washed with distilled water, and dried at room temperature for 24 h. Next, these materials were heated at 600°C for 1 h and then cooled to room temperature.

Images of the resulting materials are shown in Fig. 1(a). All of the materials were sterilized using ethylene oxide gas before use.

Scanning electron microscopy

The surface topography of the materials was observed using a field-emission scanning electron microscope (SEM) (S-4700, Hitachi, Tokyo, Japan) at an acceleration voltage of 5 kV. For observation of the cells on the material surfaces, the materials were fixed in 2% glutaraldehyde for 1 h at 2 days after seeding. The materials were rinsed gently with 0.1 M phosphate buffer at pH 7.2, dehydrated in an ethanol series, frozen in tert-butyl alcohol, freeze-dried, and sputter-coated with gold and palladium.

Surface characterization

Roughness parameters were determined using a 3-D measuring laser microscope (OLS4100, Shimadzu, Kyoto, Japan). The center of each material was measured with a measurement length of 4,000 μm. The measured parameters and their definitions were as follows: *Ra*, the average peak-to-valley distance; *Rp*, the highest peak value; and *Rz*, the highest peak to the lowest valley distance.

Wettability of the materials was assessed by measuring the contact angles of pure water on the material surfaces. A drop of pure water was gently dropped onto the surfaces, and the contact angles were measured after 10 s. This test was repeated five times for each material.

Cell culture

The materials were placed on the bottom of the wells of 12-well culture dishes. Primary mouse osteoblasts were harvested from the calvaria of 1- to 5-day-old C57/BL6 mice using a modification of a previously described protocol[24]. Calvarial bone fragments were subjected to five sequential 15 min digestions in medium containing 0.1% collagenase P (Roche Applied Science, Indianapolis, IN, USA) and 0.00125% trypsin (Sigma-Aldrich, St. Louis, MO, USA), and cell fractions 3–5 were collected. Cells were seeded at a density of 1×10^5 cells/well in 12-well tissue culture polystyrene plates containing the sample materials on the bottom. Cells were grown in osteogenic medium comprising DMEM (Sigma-Aldrich) supplemented with 10% fetal bovine serum (Tissue Culture Biologicals, Long Beach, CA, USA), 10 mM *β*-glycerophosphate (Sigma-Aldrich), 80 μg/mL ascorbic acid (Sigma-Aldrich), and 10^{-8} M dexamethasone (Sigma-Aldrich) at 37°C in a humidified atmosphere of 5% CO_2 and 95% air. The culture medium was replaced every other day. In order to separate the cells on the materials from the cells on the bottom of the culture dishes, we moved the materials to new culture dishes just before performing the following biochemical analysis: XTT assay and real-time RT-PCR analysis.

2,3-bis(2-methoxy-4-nitro-5-sulfophenyl)-2H-tetrazolium-5-carboxanilide (XTT) reduction assay

For the evaluation of cell adhesion and proliferation, the cell number was assessed by XTT (2,3-bis(2-methoxy-

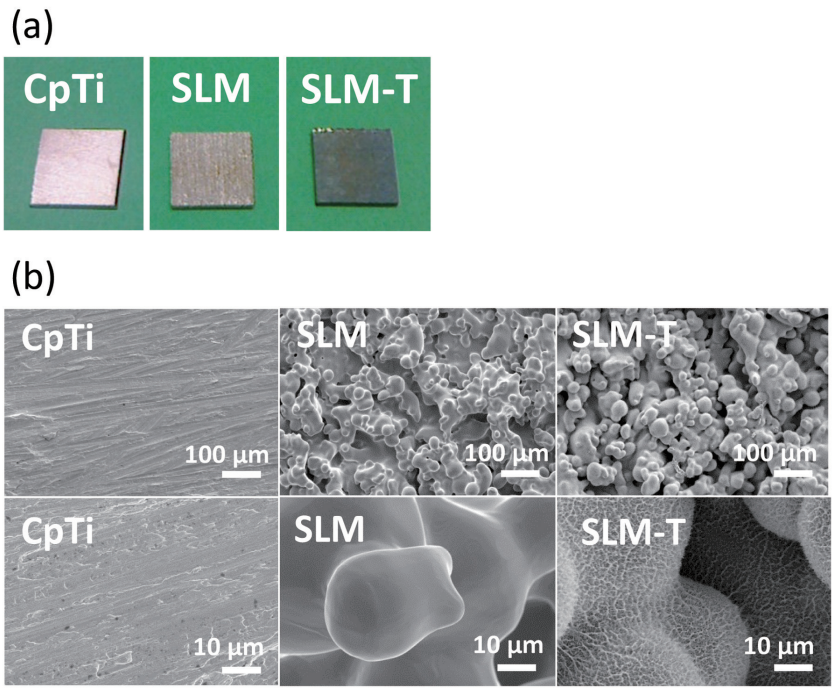

Fig. 1 (a) Representative images of the three materials evaluated in this study. From left to right: flat-rolled commercially pure titanium polished with grade 400 diamond plates (CpTi), a titanium material fabricated by selective laser melting (SLM), and a titanium material fabricated by SLM and treated with dilute HCl-treated alkali and heat treatment (SLM-T). Sample sizes were 14×14×1 mm.
(b) Scanning electron microscopic (SEM) images of the materials. The surface of the CpTi material appears flat in the magnified image. The materials fabricated by SLM had a rough surface composed of the melted and fused particles of titanium. After the bioactive treatment, nanoscale porous architectures were formed on the surface of the material.

4-nitro-5-sulfophenyl)-2H-tetrazolium-5-carboxanilide) reduction assay 2 and 7 days after seeding, as described previously[25]. Briefly, 500 µL of XTT working solution was added to each well. The cells were incubated at 37°C for 4 h, and the absorbance was measured on a microplate reader (Thermo LabSystems, Cheshire, UK). Specific absorbance was calculated as follows: specific absorbance=A450 nm (test)–A450 nm (blank)–A630 nm (test).

Confocal laser scanning imaging of cell cultures
Two days after seeding, cells were fixed by 4% paraformaldehyde in PBS for 15 min at room temperature and were permeabilized with 0.1% Triton X-100 in PBS for 10 min, then blocked using 4% FBS in PBS for 30 min. After blocking, cells were incubated with tetramethylrhodamine isothiocyanate (TRITC)-conjugated phalloidin (1:500, Invitrogen, Waltham, MA, USA) to detect actin and TO-PRO®-3 (1:2000, Invitrogen) to detect the nucleus. Observations were performed using a confocal fluorescent microscope (Nikon Instruments, Tokyo, Japan) with appropriate filters.

Real-time RT-PCR
Total RNA was extracted using the RNeasy Mini Kit (Qiagen, Hilden, Germany) according to the manufacturer's instructions. The quality of RNA was confirmed by electrophoresis using an agarose ethidium bromide gel. From each sample, 200 ng of RNA was reverse-transcribed with random primers using the Transcriptor First Strand cDNA Synthesis kit (Roche Applied Science). Real-time RT-PCR was performed to assess the expression levels of the genes alkaline phosphatase (*Alp*) and osteocalcin (*Ocn*), using the carousel-based LightCycler system (Roche Applied Science) with FastStart DNA Master SYBR Green (Roche Applied Science). The primers were as follows: *glyceraldehyde 3-phosphate dehydrogenase* (*Gapdh*), 5'-TGTCCGTCGTGGATCTGAC-3' and 5'-CCTGCTTCACCACCTTCTTG-3'; *Alp*, 5'-ACTCAGGGCAATGAGGTCAC-3' and 5'-CACCCGAGTGGTAGTCACAA-3'; and *Ocn*, 5'-AGACTCCGGCGCTACCTT-3' and 5'-CTCGTCACAAGCAGGGTTAAG-3'.

Statistical analysis
All data were expressed as mean±standard deviation (SD). Statistical evaluation was conducted using one-way analysis of variance (ANOVA) followed by *post hoc* testing (Tukey's multiple comparison test). Statistical software EZR vers.1.27[26] was used for the analysis. Results were regarded as significant when $p<0.05$.

RESULTS

Surface characteristics of the materials

Representative SEM images of the materials are shown in Fig. 1(b). The surface of the CpTi material was smooth in the magnified image. In contrast, the surface of the SLM material was extremely rough, with melted and fused particles of titanium observed. After the bioactive treatment, nanoscale porous architectures were observed on the surface of the SLM-T material in the magnified image. The corresponding roughness parameters *Ra*, *Rp*, and *Rz* are reported in Table 1. The SLM material had a larger roughness value (*Ra*=24.58 μm) than the CpTi material (*Ra*=1.02 μm). The additional application of the bioactive treatment did not change the original microscale roughness of the SLM material (*Ra*=23.50 μm for SLM-T).

The contact angles for the materials are detailed in Table 2. Both the CpTi and the untreated SLM materials had large contact angles, suggesting their hydrophobic nature (82.37° for CpTi and 89.33° for SLM). After bioactive treatment, the surface of the SLM-T material became highly hydrophilic to an immeasurable extent.

Cell observation

SEM images of cultured osteoblasts on each material 2 days after seeding are shown in Fig. 2 (a). On the CpTi material, osteoblasts were flat and widely stretched. Similarly, on the SLM material, osteoblasts

Table 1 Roughness parameters of the three materials

	Ra (μm)	*Rp* (μm)	*Rz* (μm)
CpTi	1.02	5.20	8.52
SLM	24.58	91.61	149.39
SLM-T	23.50	84.31	136.95

Ra; the average peak to valley distance, *Rp*; the highest peak value, *Rz*; the highest peak to the lowest valley distance.

Table 2 Water contact angles on the materials

	Contact angle° (±SD)
CpTi	82.37 (±0.60)
SLM	89.33 (±3.29)
SLM-T	unmeasurable*

*:Water distributed immediately after dropped.

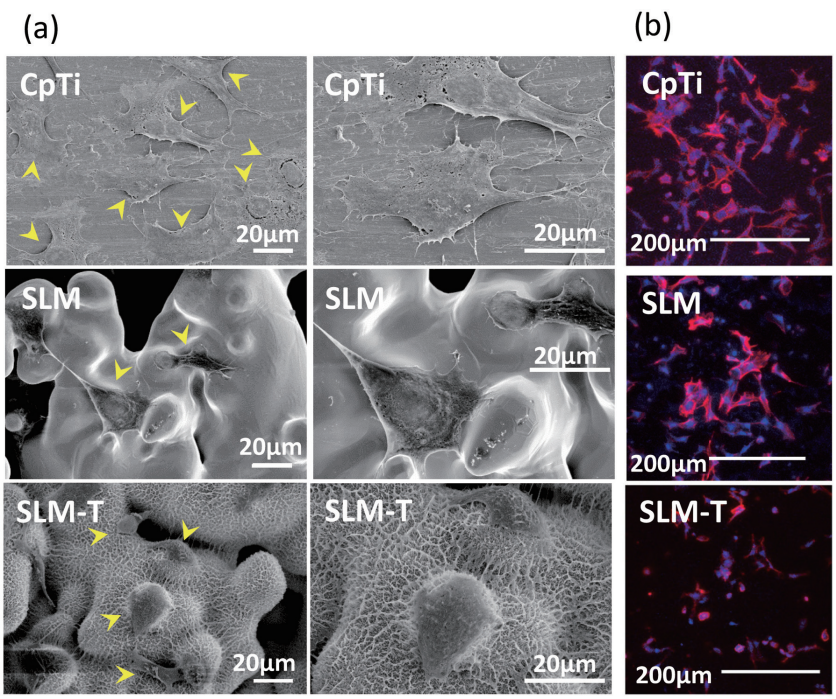

Fig. 2 (a) SEM images of the cultured osteoblasts on each material 2 days after seeding. The osteoblasts are indicated by yellow arrowheads. On the CpTi material, osteoblasts were flat and widely stretched. On the untreated material fabricated by SLM, the osteoblasts were irregularly stretched. On the treated materials fabricated by SLM (SLM-T), the osteoblasts were small and round.
(b) Fluorescent immunostaining images of the cultured osteoblasts 2 days after seeding. The actin filaments are indicated in red, and the nuclei are indicated in blue. The cell morphology observed by fluorescent immunostaining was compatible with the SEM observations.

were flat and stretched into irregular shapes, fitting the microarchitecture of the surface. On the SLM-T material, the osteoblasts were small and round. Fluorescent immunostaining images are shown in Fig. 2 (b). The actin filaments of the osteoblasts on both the CpTi and the SLM materials were clearly evident and well-stretched. On the other hand, the actin filaments of osteoblasts on the SLM-T material were less obvious, and the distribution was restricted to the vicinity of the nuclei. The fluorescent images were compatible with the SEM observations.

Cell number

The results of the XTT assays are shown in Fig. 3 (a). On day 2, the SLM and SLM-T materials had a significantly higher absorbance compared with the CpTi material (CpTi, 0.07±0.02; SLM, 0.12±0.02; SLM-T, 0.13±0.01). On day 7, the SLM-T material had a significantly lower absorbance compared with the CpTi and SLM materials (CpTi, 0.99±0.06; SLM, 0.95±0.04; SLM-T, 0.62±0.02).

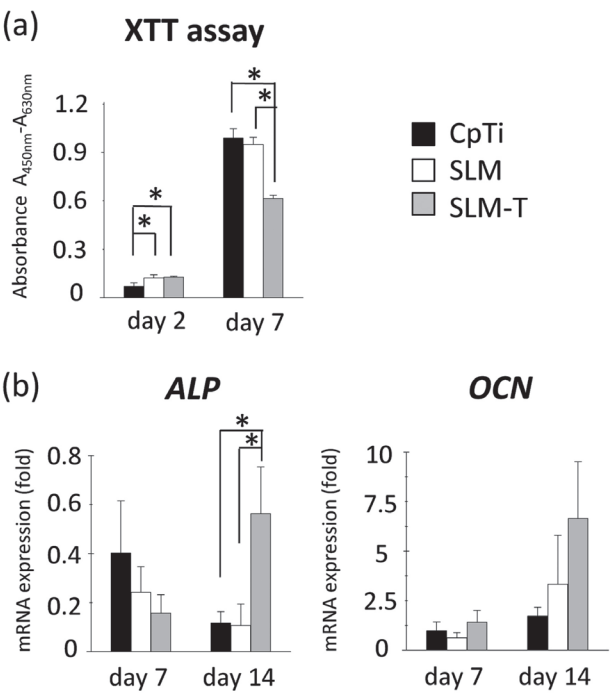

Fig. 3 (a) Cell number evaluated by XTT assay on days 2 and 7. On day 2, the cells on the materials fabricated by SLM had larger absorbance than the CpTi materials (*: $p<0.05$). No significant difference was observed between the untreated and treated materials. On day 7, the cells on the treated materials had lower absorption compared with the other two materials.
(b) The expression of osteogenic genes *ALP* and *OCN* of cultured osteoblasts on each material. On day 7, no significant differences in the expression levels of these two genes were observed between the materials. On day 14, the cells on the treated materials had a higher *ALP* expression level compared with the other two materials (*: $p<0.05$). The expression level of *OCN* was the highest for cells on the SLM-T materials, but the difference was not significant ($p>0.05$).

Osteoblast differentiation

The effects of the different materials on osteoblast differentiation were assessed by measuring the expression levels of *ALP* and *OCN* (Fig. 2 (b)). On day 7, no significant differences in the expression levels of *ALP* or *OCN* were observed between these materials (*ALP*: CpTi, 0.40±0.25; SLM, 0.24±0.12; SLM-T, 0.16±0.09. *OCN*: CpTi, 0.98±0.52; SLM, 0.62±0.31; SLM-T, 1.42±0.67). On day 14, the cells on the SLM-T material had significantly higher *ALP* expression levels compared with the other materials (CpTi, 0.12±0.05; SLM, 0.12±0.09; SLM-T, 0.56±0.22). In addition, the cells on the SLM-T material also had the highest expression levels of *OCN* on day 14 (CpTi, 1.72±0.45; SLM, 3.42±2.14; SLM-T, 6.65±2.87. $p=0.05$ for CpTi *vs.* SLM-T, $p=0.23$ for SLM *vs.* SLM-T, $p=0.63$ for CpTi *vs.* SLM), although these differences were not significant.

DISCUSSION

The surfaces of the material samples fabricated by SLM had very high roughness values compared with the flat-rolled and polished materials.

On day 2, significantly higher absorbance values obtained by XTT assay were observed for both the SLM and the SLM-T materials compared with the CpTi material. At this early time point, we could assume that this result may come from a difference in primary adhesion of the osteoblasts to the materials rather than their proliferation afterward, because the SLM and the SLM-T materials had apparently larger surface areas than the CpTi material.

After day 2, we did not observe significant differences in cell number or in osteogenic differentiation between the CpTi and untreated SLM materials. The original microscale architecture fabricated by SLM neither negatively influenced osteoblast differentiation nor enhanced it. There are many reports describing the relationship between microscale surface roughness and osteoblast differentiation. Although there is no clear consensus about the optimal microscale roughness for osteoblast differentiation, osteoblasts generally favor rough surfaces with *Ra* values of about 3–5 μm above smooth surfaces with *Ra* values <1 μm[20,27,28]. *In vivo* studies have shown that rough surfaces with *Ra* values in 3–5 μm are more suitable for osteointegration than smooth surfaces[16,17]. However, most previous reports on *in vitro* studies have focused mainly on rough surfaces with *Ra* values <5 μm. The effects of rougher surfaces on osteoblast differentiation have not received much attention. Materials with higher roughness values beyond this range did not always improve osteointegration *in vivo*[29].

Materials fabricated by additive manufacturing

methods generally have very rough surfaces because the materials are fabricated using metal powders. There have only been a few studies that have evaluated the effects of these very rough surfaces on osteoblast differentiation. In a study that evaluated Ti-6Al-4V mesh scaffolds fabricated by SLM with primary human osteoblasts, the osteoblasts on the scaffolds showed the same well-stretched morphology[30] as the osteoblasts observed on the untreated SLM material in our study, although the differentiation was not evaluated biochemically. In another study, Ponader *et al*. reported the responses of human osteoblasts to the different surfaces of Ti-6Al-4V plates fabricated by electron beam melting with different settings. In their study, the osteoblasts cultured on the rough surface (*Ra*=24.9 μm) showed the same well-spread morphology as the osteoblasts cultured on the polished and smooth surface (*Ra*=0.077 μm), and a higher cell number was observed on the smooth surface than on the rough surface on days 7 and 14[31]. In addition, they observed no significant differences in the expression levels of osteoblast-specific genes between the smooth and rough surfaces. These results are consistent with our finding that the original very rough surface of the materials fabricated by SLM did not have a promotional effect on osteoblast differentiation.

It is widely accepted that surface topography modulates cell differentiation through mechanisms similar to those of mechanotransduction[32]. Focal adhesions are formed with the material surface, and the signal is transmitted to intracellular signaling pathways *via* integrins followed by cytoskeleton organization[32-34]. The mechanisms by which different surface topographies induce different patterns of focal adhesion in osteoblast are unknown. One study showed that epithelial cells formed fewer and smaller focal adhesions on rough (*Ra*=0.58–5.09 μm) titanium surfaces than on smooth (*Ra*=0.06 μm) surfaces[35]. On the rough surfaces, the focal adhesions were localized mainly to the ridges rather than the valleys. The SLM materials used in our study were composed of round humps of melted titanium powders and had high roughness parameter values. However, as shown by SEM images, the local surfaces of these humps were very smooth. The osteoblasts stretched over the humps and valleys, but there were no sharp ridges on their surface. The lack of ridges on the surface may be a reason why no difference was observed between the SLM and CpTi materials in terms of osteoblast differentiation. However, further study is required to elucidate the relationship between the specific focal adhesion of osteoblasts on different surfaces and osteoblast differentiation.

After the application of a bioactive treatment, the SLM-T materials obtained increased wettability and nanoscale architecture on the surface. Furthermore, the osteoblasts cultured on the SLM-T material showed enhanced osteogenic differentiation as indicated by their round-cuboidal morphology[20,36,37] and the increased *ALP* expression on day 14[36,38]. We believe that the lower XTT absorbance observed for the SLM-T material on day 7 also indicates an early shift of the osteoblasts from proliferation to differentiation. Regarding the interpretation of the results of an XTT assay, the stimulation of proliferation of osteolineage cells has also been widely used as a simple indicator of the biocompatibility of materials[39-41]. However, on various types of materials, enhanced osteoblast differentiation has been observed concomitantly with decreased cell proliferation and round cell morphology[20,21,37,42]. These results are compatible with the well-described maturation process of primary osteoprogenitor cells in culture, namely that proliferating preosteoblasts in polygonal shape differentiate to matrix-synthesizing osteoblasts in cuboidal shape[36]. We therefore consider there to be no inconsistency between our results of XTT assay and our results of other evaluations.

The effects of bioactive treatment have been reported on flat material surfaces[37,43,44], and our current results indicate that the very rough surfaces fabricated by SLM also acquired a positive effect on osteoblast differentiation from bioactive treatment. The positive effects of bioactive treatments have been mainly attributed to the altered surface chemistry and charge, and subsequent apatite formation on the material *in vivo* and in a simulated body fluid[13,43,45]. In this *in vitro* study, we might assume that the nanoscale pores and increased wettability of the SLM-T material might also have had beneficial effects on osteoblast differentiation. The nanoscale pore distribution of the surface treated by dilute HCl-treated alkali and heat treatment had a broad peak below 0.1 μm and a peak near 0.5 μm[12]. There have been many studies describing various nanostructures on titanium materials, and most of them have reported positive effects on osteoblast proliferation[39]. The superposition of nanoscale structures (pore diameter ranged between 20 nm and 180 nm) on a microrough surface (*Sa*=2.20) has been reported to provide the original surface with additional benefits including the enhancement of osteogenic gene expression[46] and modification of the expression profile of integrin subunits[47] of osteoblasts.

Wettability has also been identified as an important factor affecting the control of osteogenic cell differentiation[48,49]. However, it is usually difficult to evaluate the specific contribution of wettability because wettability is strongly affected by the surface roughness and chemistry. Recent attempts to modify wettability without changing the surface microstructure and chemistry have revealed that hydrophilic surfaces modulated the expression profile of integrin subunits and enhanced osteogenic cell differentiation[50,51]. The hypothetical mechanism of the effects of hydrophilic surfaces on cell attachment and subsequent reactions is that the hydrophilicity influences the protein absorption to the material surface and prevents the entrapment of air bubbles within the surface architecture, which could interfere with protein absorption and material-cell interaction[49]. Increased wettability resulting from the bioactive treatment might have been especially beneficial for the SLM-T materials evaluated in this study, because materials fabricated by SLM have very

rough surfaces and a complex architecture that might increase the risk of entrapment of air bubbles.

Finally, although the very rough surface fabricated by SLM might be beneficial for early mechanical stability *in vivo*, our results indicate that the original surface was not effective for osteoblast differentiation. We assumed that the application of a bioactive treatment could be a promising method to promote the bone-material fixation of titanium materials with complex architectures fabricated by SLM.

CONCLUSION

The present study showed that the original very rough surface of the materials fabricated by SLM did not have a specific effect on osteoblast differentiation compared with the flat-rolled titanium materials. The application of a bioactive treatment significantly enhanced osteoblast differentiation on the SLM materials. We concluded that materials fabricated by SLM had to undergo a bioactive treatment to promote their fixation to bone.

REFERENCES

1) Murr LE, Gaytan SM, Martinez E, Medina F, Wicker RB. Next generation orthopaedic implants by additive manufacturing using electron beam melting. Int J Biomater 2012; 2012: 245727.
2) Steno B, Kokavec M, Necas L. Acetabular revision arthroplasty using trabecular titanium implants. Int Orthop 2015; 39: 389-395.
3) Hollander DA, von Walter M, Wirtz T, Sellei R, Schmidt-Rohlfing B, Paar O, Erli HJ. Structural, mechanical and in vitro characterization of individually structured Ti-6Al-4V produced by direct laser forming. Biomaterials 2006; 27: 955-963.
4) Lin CY, Wirtz T, LaMarca F, Hollister SJ. Structural and mechanical evaluations of a topology optimized titanium interbody fusion cage fabricated by selective laser melting process. J Biomed Mater Res A 2007; 83: 272-279.
5) Mullen L, Stamp RC, Brooks WK, Jones E, Sutcliffe CJ. Selective Laser Melting: a regular unit cell approach for the manufacture of porous, titanium, bone in-growth constructs, suitable for orthopedic applications. J Biomed Mater Res B Appl Biomater 2009; 89: 325-334.
6) Rotaru H, Schumacher R, Kim SG, Dinu C. Selective laser melted titanium implants: a new technique for the reconstruction of extensive zygomatic complex defects. Maxillofac Plast Reconstr Surg 2015; 29; 37: 1.
7) Rana M, Gellrich MM, Gellrich NC. Customised reconstruction of the orbital wall and engineering of selective laser melting (SLM) core implants. Br J Oral Maxillofac Surg 2015; 53: 208-209.
8) Hacking SA, Tanzer M, Harvey EJ, Krygier JJ, Bobyn JD. Relative contributions of chemistry and topography to the osseointegration of hydroxyapatite coatings. Clin Orthop Relat Res 2002; 405: 24-38.
9) Dumbleton J, Manley MT. Hydroxyapatite-coated prostheses in total hip and knee arthroplasty. J Bone Joint Surg Am 2004; 86-A: 2526-2540.
10) Park JW, Kurashima K, Tustusmi Y, An CH, Suh JY, Doi H, Nomura N, Noda K, Hanawa T. Bone healing of commercial oral implants with RGD immobilization through electrodeposited poly(ethylene glycol) in rabbit cancellous bone. Acta Biomater 2011; 7: 3222-3229.
11) Yan WQ, Nakamura T, Kobayashi M, Kim HM, Miyaji F, Kokubo T. Bonding of chemically treated titanium implants to bone. J Biomed Mater Res 1997; 37: 267-275.
12) Takemoto M, Fujibayashi S, Neo M, Suzuki J, Matsushita T, Kokubo T, Nakamura T. Osteoinductive porous titanium implants: effect of sodium removal by dilute HCl treatment. Biomaterials 2006; 27: 2682-2691.
13) Kokubo T, Pattanayak DK, Yamaguchi S, Takadama H, Matsushita T, Kawai T, Takemoto M, Fujibayashi S, Nakamura T. Positively charged bioactive Ti metal prepared by simple chemical and heat treatments. J R Soc Interface 2010; 6; 7 Suppl 5: S503-513.
14) Kawanabe K, Ise K, Goto K, Akiyama H, Nakamura T, Kaneuji A, Sugimori T, Matsumoto T. A new cementless total hip arthroplasty with bioactive titanium porous-coating by alkaline and heat treatment: average 4.8-year results. J Biomed Mater Res B Appl Biomater 2009; 90: 476-481
15) Pattanayak DK, Fukuda A, Matsushita T, Takemoto M, Fujibayashi S, Sasaki K, Nishida N, Nakamura T, Kokubo T. Bioactive Ti metal analogous to human cancellous bone: Fabrication by selective laser melting and chemical treatments. Acta Biomater 2011; 7: 1398-1406.
16) Wennerberg A, Albrektsson T. Effects of titanium surface topography on bone integration: a systematic review. Clin Oral Implants Res 2009; 20 Suppl 4:172-184.
17) Buser D, Nydegger T, Oxland T, Cochran DL, Schenk RK, Hirt HP, Snétivy D, Nolte LP. Interface shear strength of titanium implants with a sandblasted and acid-etched surface: a biomechanical study in the maxilla of miniature pigs. J Biomed Mater Res 1999; 45: 75-83.
18) Elias CN, Oshida Y, Lima JH, Muller CA. Relationship between surface properties (roughness, wettability and morphology) of titanium and dental implant removal torque. J Mech Behav Biomed Mater 2008; 1: 234-242.
19) Buser D, Janner SF, Wittneben JG, Brägger U, Ramseier CA, Salvi GE. 10-year survival and success rates of 511 titanium implants with a sandblasted and acid-etched surface: a retrospective study in 303 partially edentulous patients. Clin Implant Dent Relat Res 2012; 14: 839-851.
20) Kim HJ, Kim SH, Kim MS, Lee EJ, Oh HG, Oh WM, Park SW, Kim WJ, Lee GJ, Choi NG, Koh JT, Dinh DB, Hardin RR, Johnson K, Sylvia VL, Schmitz JP, Dean DD. Varying Ti-6Al-4V surface roughness induces different early morphologic and molecular responses in MG63 osteoblast-like cells. J Biomed Mater Res A 2005; 74: 366-373.
21) Vandrovcová M, Bačáková L. Adhesion, growth and differentiation of osteoblasts on surface-modified materials developed for bone implants. Physiol Res 2011; 60: 403-417.
22) Fukuda A, Takemoto M, Saito T, Fujibayashi S, Neo M, Pattanayak DK, Matsushita T, Sasaki K, Nishida N, Kokubo T, Nakamura T. Osteoinduction of porous Ti implants with a channel structure fabricated by selective laser melting. Acta Biomater 2011; 7: 2327-2336.
23) Pattanayak DK, Kawai T, Matsushita T, Takadama H, Nakamura T, Kokubo T. Effect of HCl concentrations on apatite-forming ability of NaOH-HCl- and heat-treated titanium metal. J Mater Sci Mater Med 2009; 20: 2401-2411.
24) Wong GL, Cohn DV. Target cells in bone for parathormone and calcitonin are different: enrichment for each cell type by sequential digestion of mouse calvaria and selective adhesion to polymeric surfaces. Proc Natl Acad Sci USA 1975; 72: 3167-3171
25) Roehm NW, Rodgers GH, Hatfield SM, Glasebrook AL. An improved colorimetric assay for cell proliferation and viability utilizing the tetrazolium salt XTT. J Immunol Methods 1991; 142: 257-265
26) Kanda Y. Investigation of the freely available easy-to-use software 'EZR' for medical statistics. Bone Marrow Transplant 2013; 48: 452-458.
27) Gittens RA, Olivares-Navarrete R, Cheng A, Anderson DM,

McLachlan T, Stephan I, Geis-Gerstorfer J, Sandhage KH, Fedorov AG, Rupp F, Boyan BD, Tannenbaum R, Schwartz Z. The roles of titanium surface micro/nanotopography and wettability on the differential response of human osteoblast lineage cells. Acta Biomater 2013; 9: 6268-6277.
28) Bächle M, Kohal RJ. A systematic review of the influence of different titanium surfaces on proliferation, differentiation and protein synthesis of osteoblast-like MG63 cells. Clin Oral Implants Res 2004;15: 683-692.
29) Vercaigne S, Wolke JG, Naert I, Jansen JA. Histomorphometrical and mechanical evaluation of titanium plasma-spray-coated implants placed in the cortical bone of goats. J Biomed Mater Res 1998; 41: 41-48.
30) Warnke PH, Douglas T, Wollny P, Sherry E, Steiner M, Galonska S, Becker ST, Springer IN, Wiltfang J, Sivananthan S. Rapid prototyping: porous titanium alloy scaffolds produced by selective laser melting for bone tissue engineering. Tissue Eng Part C Methods 2009; 15:115-124.
31) Ponader S, Vairaktaris E, Heinl P, Wilmowsky CV, Rottmair A, Körner C, Singer RF, Holst S, Schlegel KA, Neukam FW, Nkenke E. Effects of topographical surface modifications of electron beam melted Ti-6Al-4V titanium on human fetal osteoblasts. J Biomed Mater Res A 2008; 84: 1111-1119.
32) Dalby MJ. Topographically induced direct cell mechanotransduction. Med Eng Phys 2005; 27: 730-742.
33) Wang W, Zhao L, Ma Q, Wang Q, Chu PK, Zhang Y. The role of the Wnt/β-catenin pathway in the effect of implant topography on MG63 differentiation. Biomaterials 2012; 33: 7993-8002.
34) Wang W, Liu Q, Zhang Y, Zhao L. Involvement of ILK/ERK1/2 and ILK/p38 pathways in mediating the enhanced osteoblast differentiation by micro/nanotopography. Acta Biomater 2014; 10: 3705-3715.
35) Baharloo B, Textor M, Brunette DM. Substratum roughness alters the growth, area, and focal adhesions of epithelial cells, and their proximity to titanium surfaces. J Biomed Mater Res A 2005; 74: 12-22.
36) Malaval L, Liu F, Roche P, Aubin JE. Kinetics of osteoprogenitor proliferation and osteoblast differentiation in vitro. J Cell Biochem 1999; 74: 616-627.
37) Tsukanaka M, Yamamoto K, Fujibayashi S, Pattanayak DK, Matsushita T, Kokubo T, Matsuda S, Akiyama H. Evaluation of bioactivity of alkali- and heat-treated titanium using fluorescent mouse osteoblasts. J Bone Miner Metab 2014; 32: 660-670.
38) Hoemann CD, El-Gabalawy H, McKee MD. In vitro osteogenesis assays: influence of the primary cell source on alkaline phosphatase activity and mineralization. Pathol Biol (Paris) 2009; 57: 318-323.
39) Goldman M, Juodzbalys G, Vilkinis V. Titanium surfaces with nanostructures influence on osteoblasts proliferation: a systematic review. J Oral Maxillofac Res 2014; 5: e1.
40) Estrin Y, Kasper C, Diederichs S, Lapovok R. Accelerated growth of preosteoblastic cells on ultrafine grained titanium. J Biomed Mater Res A 2009; 90: 1239-1242.
41) Kalantari SM, Arabi H, Mirdamadi S, Mirsalehi SA. Biocompatibility and compressive properties of Ti-6Al-4V scaffolds having Mg element. J Mech Behav Biomed Mater 2015; 48: 183-191.
42) Schwartz Z, Lohmann CH, Oefinger J, Bonewald LF, Dean DD, Boyan BD. Implant surface characteristics modulate differentiation behavior of cells in the osteoblastic lineage. Adv Dent Res 1999; 13: 38-48.
43) Nishio K, Neo M, Akiyama H, Nishiguchi S, Kim HM, Kokubo T, Nakamura T. The effect of alkali- and heat-treated titanium and apatite-formed titanium on osteoblastic differentiation of bone marrow cells. J Biomed Mater Res 2000; 52: 652-661
44) Isaac J, Galtayries A, Kizuki T, Kokubo T, Berda A, Sautier JM. Bioengineered titanium surfaces affect the gene-expression and phenotypic response of osteoprogenitor cells derived from mouse calvarial bones. Eur Cell Mater 2010; 20: 178-196
45) Neo M, Nakamura T, Ohtsuki C, Kokubo T, Yamamuro T. Apatite formation on three kinds of bioactive material at an early stage in vivo: a comparative study by transmission electron microscopy. J Biomed Mater Res 1993; 27: 999-1006.
46) Gittens RA, Olivares-Navarrete R, McLachlan T, Cai Y, Hyzy SL, Schneider JM, Schwartz Z, Sandhage KH, Boyan BD. Differential responses of osteoblast lineage cells to nanotopographically-modified, microroughened titanium-aluminum-vanadium alloy surfaces. Biomaterials 2012; 33: 8986-8994.
47) Gittens RA, Olivares-Navarrete R, Hyzy SL, Sandhage KH, Schwartz Z, Boyan BD. Superposition of nanostructures on microrough titanium-aluminum-vanadium alloy surfaces results in an altered integrin expression profile in osteoblasts. Connect Tissue Res 2014; 55 Suppl 1: 164-168.
48) Rupp F, Gittens RA, Scheideler L, Marmur A, Boyan BD, Schwartz Z, Geis-Gerstorfer J. A review on the wettability of dental implant surfaces I: theoretical and experimental aspects. Acta Biomater 2014; 10: 2894-2906.
49) Gittens RA, Scheideler L, Rupp F, Hyzy SL, Geis-Gerstorfer J, Schwartz Z, Boyan BD. A review on the wettability of dental implant surfaces II: Biological and clinical aspects. Acta Biomater 2014; 10: 2907-2918.
50) Park JH, Wasilewski CE, Almodovar N, Olivares-Navarrete R, Boyan BD, Tannenbaum R, Schwartz Z. The responses to surface wettability gradients induced by chitosan nanofilms on microtextured titanium mediated by specific integrin receptors. Biomaterials 2012; 33: 7386-7393.
51) Liskova J, Babchenko O, Varga M, Kromka A, Hadraba D, Svindrych Z, Burdikova Z, Bacakova L. Osteogenic cell differentiation on H-terminated and O-terminated nanocrystalline diamond films. Int J Nanomed 2015; 10: 869-884.